Catena 266 (2026) 109951

Contents lists available at ScienceDirect

Catena

journal homepage: www.elsevier.com/locate/catena

Competitive equilibrium between carbon loss and sequestration driven by erosion: Stratified responses of microbial metabolism and mineral protection

Mengni Li [a], Yulong Shi [a], Runyu Xue [a,c], Jeroen Meersmans [b], Qingwen Zhang [a,*]

[a] Agricultural Clean Watershed Research Group, Institute of Environment and Sustainable Development in Agriculture, Chinese Academy of Agricultural Sciences/Key Laboratory of Agricultural and Rural Eco-Environment, Ministry of Agriculture and Rural Affairs, Beijing 100081, China
[b] Gembloux Agro-BioTech, Biosystem Engineering, Soil–Water–Plant Exchanges, University of Liege, Passage des Déportés, Gembloux, Belgium
[c] College of Resources and Environment, Qingdao Agricultural University, Qingdao 266109, China

ARTICLE INFO

Dataset link: Competitive Equilibrium Between Carbon Loss and Sequestration driven by Erosion: Stratified Responses of Microbial Metabolism and Mineral Protection (Original data)

Keywords:
Soil erosion
Carbon fractionation
Microbial carbon use efficiency
Carbon mineralization
Sediment selectivity

ABSTRACT

Soil erosion drives the redistribution of soil organic carbon (SOC) through transportation and deposition processes, yet its underlying mechanisms in shaping the carbon source/sink patterns on slopes remain inadequately understood. Prevailing studies have predominantly focused on the physical translocation effects of erosion, overlooking the biologically-driven priming mineralization. The differential transport and burial of particulate organic carbon (POC) and mineral-associated organic carbon (MAOC) induced by erosion may form a physical carbon sink; however, the synergistic mechanisms between physical protection and biological metabolic processes are still unclear. To address this critical knowledge gap, this study investigated a gentle slope in the Black Soil Region of Northeast China. We measured the contents of SOC fractions (SOC, POC, and MAOC), soil extracellular enzyme activities (BG, and NAG+LAP), and microbial carbon use efficiency (CUE) in topsoil (0–20 cm) and subsoil (20–40 cm) layers along typical upper and lower slope positions. Partial least squares path modeling (PLS-PM) analysis results indicated that the upper zones suffered from a loss of labile POC due to selective erosion, leading to microbial substrate scarcity and a decline in CUE, thereby exacerbating carbon loss. In contrast, lower zones facilitated the enrichment of stable MAOC through mineral protection mechanisms, concomitant with an increase in CUE, creating a local carbon sink. Simultaneously, the vertical migration of carbon contributed to the formation of a relatively stable MAOC pool in the subsoil, partially offsetting erosion-induced carbon release. This study reveals that the redistribution of particulate organic carbon (POC) and mineral-associated organic carbon (MAOC) across eroded landscapes, coupled with microbial metabolic adaptation, governs the carbon source/sink dynamics along the slope. Future assessments of the carbon budget under soil erosion must concurrently quantify the losses from physical translocation and the sequestration driven by mineral-biological synergy to systematically decipher the response pathways of the carbon cycle to erosion.

1. Introduction

Soil constitutes the largest terrestrial carbon pool, and the dynamics of its organic carbon (SOC) significantly influence the global carbon cycle. Nevertheless, the mechanisms governing SOC mineralization and sequestration during erosion and deposition processes remain insufficiently elucidated. Soil erosion, through processes including deaggloeration, collapse, transport, redistribution, and deposition, profoundly disturbs SOC stability and its sequestration capacity (Doetterl et al., 2016). In recent years, SOC has been broadly categorized into particulate organic carbon (POC; primarily derived from plant debris, >53 μm) and mineral-associated organic carbon (MAOC; organo-mineral complexes, <53 μm) (Kramer and Chadwick, 2018; Shi et al., 2024). This partitioning framework offers an effective approach to unravel the pathways and stability of SOC accumulation (Cotrufo et al., 2019; Lavallee et al., 2020). POC and MAOC exhibit distinct formation pathways, stability, and driving factors. POC accumulation is typically associated with increased plant carbon input (Tang et al., 2023; Ye et al., 2018) or suppressed microbial decomposition (Chen et al., 2020), whereas its depletion often coincides with decreased microbial CUE and

* Corresponding author.
E-mail address: zhangqingwen@caas.cn (Q. Zhang).

https://doi.org/10.1016/j.catena.2026.109951
Received 16 November 2025; Received in revised form 7 January 2026; Accepted 20 February 2026
Available online 26 February 2026

enhanced enzyme activities. Conversely, MAOC is primarily stabilized through sorption onto mineral surfaces (Li et al., 2024b), For instance, the enrichment of fine particles, high specific surface area, and silt-plus-clay content in depositional zones significantly enhance SOC retention capacity (Shi et al., 2024). The transport and redeposition of fine particles and SOC during erosion profoundly impact carbon stability and sequestration potential. In depositional areas, SOC can be stabilized over the long term through re-aggregation, physical isolation, and chemical encapsulation/protection by minerals (Yu et al., 2022). In summary, POC, being more physically exposed, is prone to mineralization and represents a more labile carbon pool, whereas MAOC, protected by minerals, exhibits higher stability and a longer turnover time (Zhang et al., 2024). Changes in these SOC fractions are more indicative of soil carbon dynamics than total SOC content. Therefore, investigating the spatial distribution and transformation mechanisms of SOC fractions on eroded slopes is of paramount scientific importance for revealing the pathways regulating soil carbon accumulation and stability.

The SOC balance is a core component of the terrestrial carbon cycle, in which microbial activity plays a key regulatory role. Microbial carbon use efficiency (CUE), defined as the proportion of assimilated carbon allocated to biomass synthesis versus respiration, directly regulates SOC accumulation and decomposition (Manzoni et al., 2017; Tao et al., 2023; Xu et al., 2017). CUE provides a physiological-ecological perspective on microbial carbon allocation strategies between growth (biomass production) and respiration (CO_2 emission), serving as a crucial parameter for understanding SOC dynamics (Tao et al., 2023). While some studies posit that higher CUE facilitates SOC stabilization and accumulation by channeling more carbon into microbial biomass and its residues (Frey et al., 2013; Kallenbach et al., 2016), others suggest that high CUE may coincide with enhanced microbial activity and extracellular enzyme (EE) secretion, potentially accelerating SOC decomposition, thus exerting a dual regulatory effect on the soil carbon pool (Ren et al., 2024). Under anthropogenic disturbances like intensive agricultural practices, soil degradation often accompanies persistent SOC loss. Restoring soil carbon stocks necessitates a deep understanding of microbial-mediated carbon allocation mechanisms, particularly the role of CUE in balancing carbon accumulation and release on erosion-affected slopes. Consequently, elucidating the regulatory mechanism of CUE on soil carbon cycling in eroded landscapes is vital for predicting changes in soil carbon sink functionality under land management and global change scenarios.

While much of the existing literature focuses on the physical redistribution of SOC during erosion, the biological drivers of mineralization and sequestration, particularly the role of microbial metabolism (e.g., CUE and enzyme secretion), remain underexplored. This knowledge gap is particularly critical in ecologically and agriculturally vital regions facing severe erosion. The Black Soil Region of Northeast China, a critical commodity grain base covering 1.09 million square kilometers, with typical black soil arable land covering 18.533 million hectares and contributing over 33% of the nation's grain output (*Report of the Protection and Utilization of Black Soil in China 2021*, 2022), is characterized by deep, fertile soils with historically high topsoil SOC content (averaging 30–50 g kg^{-1}) (Sorokin et al., 2021), indicating significant carbon sink potential. However, over the past three decades, long-term intensive cultivation and severe slope erosion have led to sustained degradation of natural fertility, accelerated soil organic matter (SOM) mineralization, and expanding soil and water loss areas, threatening the sustainable use of black soil resources and undermining their role in climate change mitigation. Regarding erosion-induced carbon loss, traditional research relying on bulk SOC measurements often perceives erosion as a net carbon source, attributing carbon loss to accelerated mineralization and lateral transport (Lal, 2003). However, growing evidence suggests that erosion-deposition systems can function as transient carbon sinks. While erosion removes labile POC from its original setting into aquatic systems, MAOC can be buried and relatively stabilized in depositional zones (Berhe et al., 2018; Wang et al., 2020). This mechanism is crucial for re-evaluating the carbon cycle paradigm under erosion. Currently, a systematic understanding of how erosion drives the spatial redistribution of SOC fractions (especially POC and MAOC) and the regulatory role of microbial metabolic processes (CUE) in carbon sequestration is still lacking. Therefore, deeply uncovering the response mechanisms of SOC fraction transport, transformation, and stability under erosion is urgently needed for accurately assessing the regional carbon balance and promoting sustainable land management in the Black Soil Region.

This study aims to reveal the mechanisms by which soil erosion influences SOC fractions (POC, MAOC), extracellular enzyme activities (EEAs: BG, NAG+LAP), and microbial CUE, and their synergistic roles in regulating SOC dynamics. The specific objectives are: (1) to quantify the spatial differentiation of carbon fractions (POC, MAOC) along an erosion slope; (2) to elucidate the response characteristics of microbial CUE along the erosional *catena*; and (3) to systematically analyze the coupled effects of carbon fraction redistribution and microbial metabolic efficiency on SOC accumulation. By collecting soil samples from a typical slope, systematically measuring SOC, POC, MAOC contents, EEAs, and microbial CUE, and constructing a SEM, this research seeks to uncover the physico-biological synergistic processes governing the carbon cycle under erosion. We hypothesize that: (1) Soil erosion will drive significant spatial differentiation of labile (POC) and stable (MAOC) carbon pools along the slope; (2) In lower zones, SOC input and burial processes will trigger adaptive metabolic responses in microbes; (3) Along the erosional slope, SOC and CUE will exhibit a positive synergistic relationship—lower zones can achieve carbon sequestration through mineral protection (MAOC accumulation) and efficient microbial carbon conversion (high CUE), thereby partially counteracting the carbon source effect of upper slopes; (4) The mechanisms regulating SOC dynamics will show depth-dependent stratification, with microbial metabolic processes dominating in the topsoil and mineral protection of MAOC being more critical in the subsoil.

2. Materials and methods

2.1. Study site

This study was conducted in the Hongxing Farm, located in Bei'an City, Heilongjiang Province (48°02′N-48°17′N, 126°47′E-127°15′E). The region experiences a cold temperate continental monsoon climate, characterized by a long, cold winter and a short, hot, rainy summer. The mean annual precipitation is 555.3 mm, predominantly occurring as intense, short-duration storms concentrated in July, August, and September. Approximately 60% of the agricultural land in this area consists of sloping farmland (gradient <10°). (An et al., 2014; Shen et al., 2023). Soil erosion rates, estimated by measuring ^{137}Cs activity, indicate that the area is primarily subjected to light erosion (Gao et al., 2024; Li et al., 2025). The slopes in the study area typically range from 500 to 1000 m in length with gradients of 3° to 8°, showing clear signs of soil erosion and deposition. The dominant soil type is meadow black soil, classified as Isohumosols according to the Chinese Soil Taxonomy (equivalent to Mollisols in the US Soil Taxonomy) with a loam clay texture (Liu et al., 2022; Wang et al., 2022). The primary cropping system is a maize-soybean rotation.

2.2. Experimental design and sample collection

The investigation was carried out on a representative long, gentle slope (300 m length, 200 m width, 5° gradient) within the Black Soil Region, which is significantly affected by water erosion. To minimize recent anthropogenic disturbance, soil sampling was conducted in September 2022, prior to crop harvest. The sampling strategy was designed based on ^{137}Cs tracer data and soil profile morphology to clearly distinguish between the key landscape positions: the upper zones with average soil erosion rates of 5087.53 t km^{-2} a^{-1} and the lower

zones with average soil erosion rates of 1282.06 t km^{-2} a^{-1} (Gao et al., 2024; Li et al., 2025). At each sampling point, soil samples were collected from the 0–20 cm and 20–40 cm depth layers. To provide triplicates, two additional sampling spots were established 1 m upslope and downslope from each central point, resulting in a total of 30 samples. The coefficient of variation (CV) data of soil particle fractions: the CVs of clay, silt, and sand in the lower zones are 17.17%, 8.41%, and 14.28%, respectively, all significantly higher than those in the upper zones (7.70%, 3.18%, and 9.11%). To better capture the potentially higher spatial heterogeneity in the lower zones, three sampling points were established there, compared to two points in the more homogeneous upper zones, ensuring sample representativeness. Each collected sample was split into two subsamples: one was air-dried, sieved (2 mm and 0.15 mm), and used for the determination of SOC and its fractions, as well as laboratory incubation experiments; the other was immediately stored on dry ice and subsequently preserved at −20 °C for the analysis of soil EEAs.

2.3. SOC fraction and soil physicochemical analyses

The SOC content of all samples was measured using an N/C analyzer (multi N/C 2100S, Analytik Jena, Germany) via the dry combustion method (Nelson and Sommers, 1996). POC and MAOC were separated by a physical fractionation procedure. Briefly, 10 g of soil was placed in a 50-mL centrifuge tube with 50 mL of 5 *g* L^{-1} sodium hexametaphosphate solution as a dispersing agent. The tubes were shaken on a reciprocal shaker at 180 rpm for 18 h to ensure complete dispersion. The soil suspension was then transferred onto a 53-μm sieve and washed with a continuous flow of deionized water until the effluent ran clear. The two fractions retained on the sieve (>53 μm, POC) and passing through it (<53 μm, MAOC) were collected into pre-weighed aluminum boxes, dried at 60 °C for 24 h, and weighed (Marriott and Wander, 2006). Methods for determining soil enzyme activity and cumulative mineralization (C_m) can be found in our previous article (Li et al., 2024a).

2.4. Carbon use efficiency from stoichiometry theory (CUE)

Carbon use efficiency ($CUE_{C:N}$) was calculated based on stoichiometry theory. The underlying principle assumes that microbial CUE is regulated by microbial biomass, substrate stoichiometric imbalance, and enzyme activities. When microbes face nutrient limitations, they secrete specific enzymes to decompose substrates to acquire needed nutrients, thereby altering their CUE (Mercer et al., 2025). This approach offers distinct advantages, it is based on a reasonable assumption of microbial elemental stoichiometric allocation at the whole-community scale (microbes allocate carbon to produce enzymes for nutrient acquisition with appropriate elemental ratios when growing on plant detritus), which aligns with the study's focus on microbial metabolic mechanisms in eroded sloping soils. It only requires a limited number of parameters (e.g., C/N/P-acquiring enzyme activities, C:N:P composition of substrates and microbial biomass) that can be constrained by existing observations, making it more operationally feasible (He et al., 2024; Schimel et al., 2022). $CUE_{C:N}$ was calculated using the following equations::

$$DC_{C:N} = \left(\frac{MB_{C:N}}{S_{C:N}}\right)\left(\frac{1}{EEA_{C:N}}\right)\# \quad (1)$$

$$EEA_{C:N} = \frac{BG}{LAP + NAG}\# \quad (2)$$

$$CUE_{C:N} = CUE_{max}\left(\frac{DC_{C:N}}{DC_{C:N} + K}\right)\# \quad (3)$$

where $DC_{C:N}$ is represents the carbon-nitrogen decoupling degree, indicating the microbial resource acquisition response to the disparity between microbial elemental stoichiometry (MBC:MBN) and that of the available substrate (SOC:TN or DOC:DON), $MB_{C:N}$ is microbial elemental stoichiometry (MBC:MBN), $S_{C:N}$ is Carbon-to-nitrogen ratio of the soil matrix (SOC:TN or DOC:DON), $EEA_{C:N}$ is the ratio of the carbon-acquiring enzyme (β-glucosidase, BG) to the nitrogen-acquiring enzymes (Leucine aminopeptidase + β-*N*-acetylglucosaminidase, LAP+NAG), reflecting microbial capacity to acquire nutrients from the substrate. CUE_{max} is the maximum CUE, was set at 0.6 based on thermodynamic constraints (Roels, 1980); *K* is the half-saturation constant, representing the threshold of microbial response to stoichiometric imbalance.

2.5. Date analysis

The data obtained from the experiment were organized and analyzed using Microsoft Excel 2024. Prior to analysis, the normality of all data was checked using histograms and the Kolmogorov-Smirnov test, and homoscedasticity was verified using Bartlett's test. Data that did not meet the assumptions of normality or homoscedasticity were natural-log transformed. *t*-tests were used to compare the differences in SOC and its fractions, cumulative carbon mineralization (C_m), EEAs, and CUE between different slope positions within the 0–40 cm soil layer. Linear regressions were employed to analyze the relationships between SOC fractions and CUE or C_m. Partial Least Squares Path Modeling (PLS-PM) was used to identify the potential pathways regulating SOC mineralization and sequestration in the eroded sloping farmland. All statistical analyses were performed using R software (version 4.5.1), primarily utilizing the packages ggplot2, plspm, lme4, and glmm.hp.

3. Results

3.1. Spatial variation of SOC and its fractions

SOC, POC, and MAOC contents exhibited significant variations with slope position and soil depth ($P < 0.05$). In the 0–20 cm layer, SOC content in lower zones (range: 31.57–35.06 g kg^{-1}) was significantly higher than that in upper zones (range: 23.60–27.15 g kg^{-1}) ($P < 0.05$, Fig. 1a). A consistent trend was observed in the 20–40 cm layer, where SOC content in lower zones (range: 20.08–29.92 g kg^{-1}) significantly exceeded that in upper zones (range: 13.80–15.99 g kg^{-1}) ($P < 0.05$, Fig. 1b).

The spatial distribution patterns of POC and MAOC aligned with that of SOC (Fig. 1a, b). POC content ranges were 3.83–10.10 g kg^{-1} and 1.00–3.18 g kg^{-1} in the 0–20 cm and 20–40 cm layers, respectively, with significantly higher values at the upper zones compared to the lower zones ($P < 0.05$, Fig. 1a, b). MAOC, being the dominant component of SOC, ranged from 15.15 to 27.12 g kg^{-1} in the 0–20 cm layer and 12.56–26.53 g kg^{-1} in the 20–40 cm layer across the slope. In the 0–20 cm layer, MAOC content was significantly higher at the lower zones than at the upper zones ($P < 0.05$, Fig. 1a), a trend that persisted in the 20–40 cm layer ($P < 0.05$, Fig. 1b).

Linear regression analysis revealed significant positive correlations between MAOC and SOC in both soil layers ($P < 0.05$, Fig. 1c). A significant positive relationship was also found between POC and SOC in the 0–20 cm layer ($P < 0.05$, Fig. 1d).

3.2. Organic carbon mineralization across slope positions

Cumulative mineralization (Cm) showed significant spatial variation between slope positions and soil depths (Fig. 2). Overall, Cm values were significantly higher in the 0–20 cm layer than in the 20–40 cm layer ($P < 0.05$, Fig. 2a, b), indicating greater mineralization activity in the topsoil. Laterally along the slope, Cm was distinctly higher at the upper zones compared to the lower zones. In the 0–20 cm layer, Cm was significantly greater at the severely eroded upper zones than at the lower zones ($P < 0.05$, Fig. 2a). However, in the 20–40 cm layer, no significant

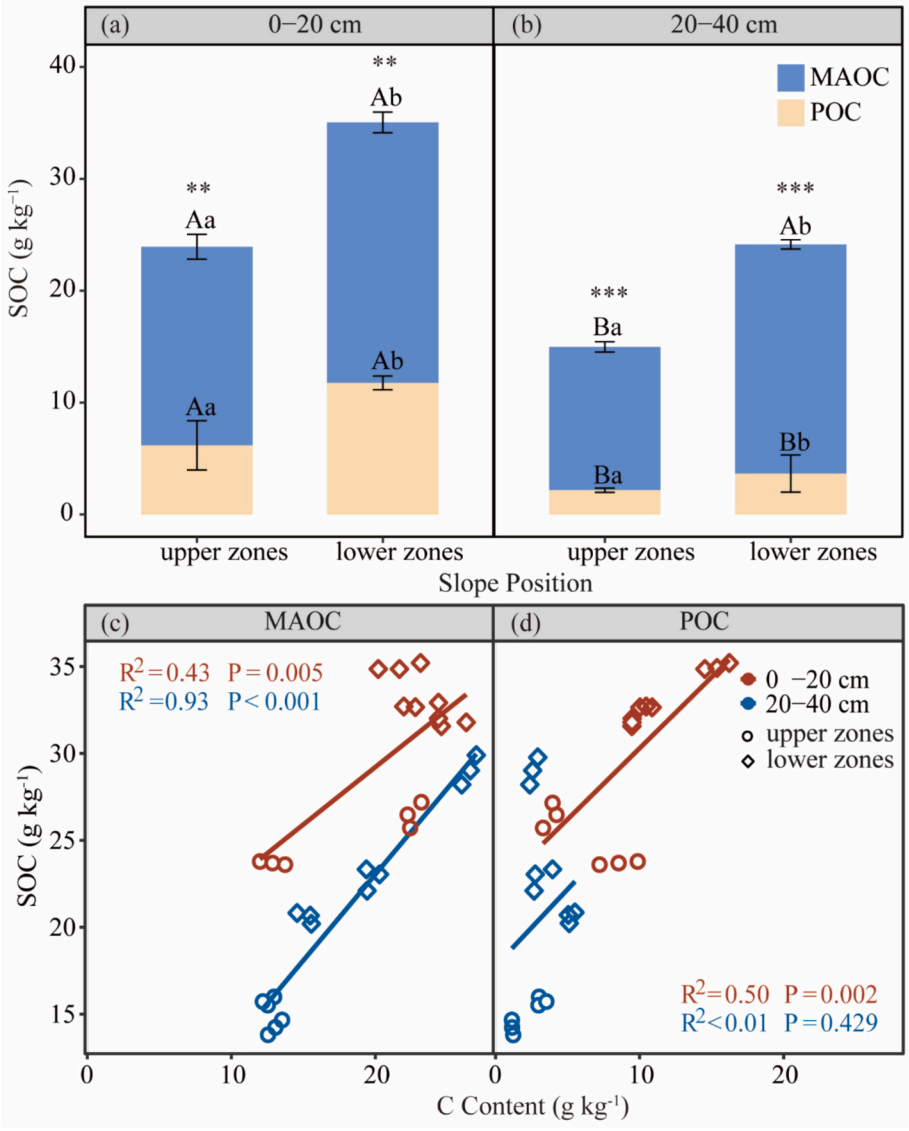

Fig. 1. Vertical and lateral distribution of POC and MAOC at different slope positions (a, b) and their relationships with SOC (c, d). Different capital letters indicate significant differences between distinct soil layers, while different lowercase letters indicate significant differences between distinct slope positions, The asterisk (*) indicates significant differences among various C fractions. * $P < 0.05$; ** $P < 0.01$; *** $P < 0.001$. SOC: Soil organic carbon; POC: particulate organic carbon; MAOC: Mineral-associated organic carbon.

difference in Cm was observed between the upper and lower zones ($P > 0.05$, Fig. 2b), with values ranging between 121.3 and 206.7 mg kg^{-1}.

3.3. Extracellular enzyme activities and carbon use efficiency

Extracellular enzyme activities (EEAs) differed significantly between slope positions and soil depths ($P < 0.05$, Fig. 3). Enzyme activities in the topsoil were significantly higher than in the subsoil ($P < 0.05$, Fig. 3a-d). Significant differences in BG and (NAG+LAP) activities were also detected between the upper and lower zones ($P < 0.05$, Fig. 3a-d).

CUE demonstrated significant spatial heterogeneity along the slope and vertical stratification (Fig. 3e, f). CUE values in the 0–20 cm layer (range: 0.08–0.20) were significantly higher than those in the 20–40 cm layer (range: 0.02–0.07). Within both soil layers, CUE was significantly higher at the lower zones compared to the upper zones ($P < 0.05$, Fig. 3e, f).

3.4. Relationships among carbon fractions, CUE, and mineralization

Linear regression analysis revealed depth-dependent relationships between carbon fractions, EEAs, Cm, and CUE (Fig. 4). In the 0–20 cm layer, Cm showed significant negative correlations with MAOC and SOC ($P < 0.05$, Fig. 4). MAOC explained more Cm variation ($R^2 = 0.39$) than total SOC ($R^2 = 0.31$). Cm was also negatively correlated with NAG+LAP ($P < 0.05$, Fig. 4). Conversely, CUE was positively correlated with POC and SOC ($P < 0.05$, Fig. 4), and negatively correlated with NAG+LAP ($P < 0.05$, Fig. 4).

In the 20–40 cm layer, the relationship between carbon fractions and Cm shifted. Cm exhibited a significant positive correlation with POC ($P < 0.05$, Fig. 4) but no significant correlation with any EEAs ($P > 0.05$, Fig. 4). CUE was positively correlated with SOC and NAG+LAP ($P < 0.05$, Fig. 4).

The relationship between C fractions and EEAs varies notably between soil layers (Fig. 5). Both BG and NAG+LAP showed significant positive correlations with MAOC in both soil layers ($P < 0.05$, Fig. 5). BG correlated positively with POC in the 0–20 cm layer ($P < 0.05$, Fig. 5),

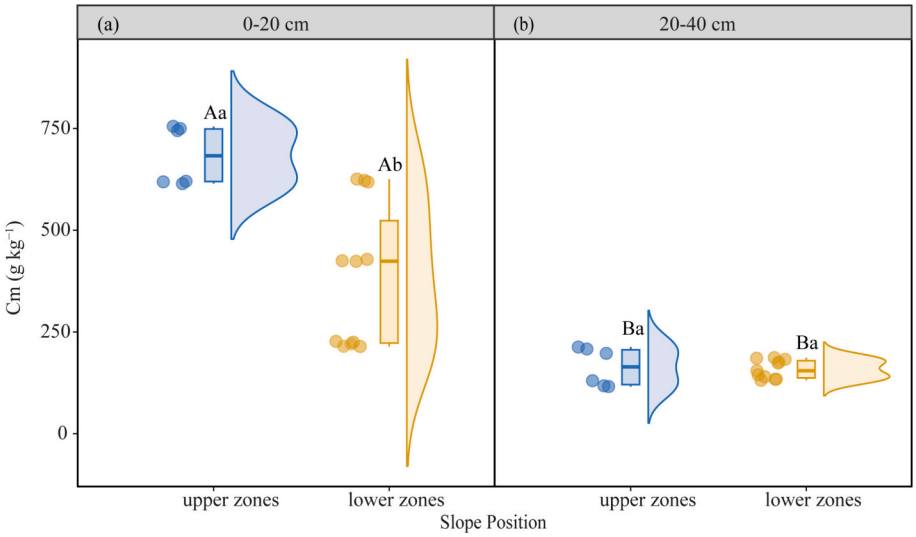

Fig. 2. Vertical and lateral distribution of Cm at different slope positions (a, b). Cm: cumulative mineralization. Different capital letters indicate significant differences between distinct soil layers, while different lowercase letters indicate significant differences between distinct slope positions.

but no significant correlations between NAG+LAP and POC were observed in 20–40 cm ($P > 0.05$, Fig. 5). (See Fig. 5.)

The relationship between CUE and Cm also differed significantly between soil layers (Fig. 6). A significant negative correlation was found between Cm and CUE in the 0–20 cm layer ($P < 0.05$, Fig. 6a). In contrast, no significant correlation was observed in the 20–40 cm layer ($P > 0.05$, Fig. 6b).

3.5. Pathways governing SOC mineralization and sequestration

Partial Least Squares Path Modeling (PLS-PM) results (Fig. 7) elucidated the key drivers and their pathways influencing SOC dynamics in the eroded slope system. Both layer-specific models had good goodness-of-fit (0–20 cm GoF = 0.731; 20–40 cm GoF = 0.717), clearly indicating that SOC accumulation is co-regulated by erosion, carbon fractions, EEs, CUE, and Cm. Path analysis identified erosion as the primary driver, exerting significant direct negative effects on POC, EEAs, and Cm. In the 0–20 cm layer, erosion indirectly influenced carbon loss by first reducing EEAs, which subsequently promoted higher CUE, thereby mitigating carbon loss. MAOC promoted EEAs, which in turn significantly enhanced microbial CUE, ultimately influencing SOC accumulation. Notably, microbial metabolic processes contributed more prominently to SOC in the topsoil (0–20 cm), whereas the direct protective role of carbon fractions (e.g., MAOC) was more critical in the subsoil (20–40 cm). These results confirm the SOC balance on eroded slopes reflects a trade-off: between erosion-induced carbon loss, and sequestration driven by mineral protection and efficient microbial conversion. This mechanism shows distinct depth-dependent stratification.

4. Discussion

4.1. Impact of erosion on soil organic carbon fractions

Soil erosion significantly drove the spatial redistribution of particulate organic carbon (POC) and mineral-associated organic carbon (MAOC) through selective transport processes, resulting in distinct vertical (profile) and lateral (slope) differentiations in their content and proportions (Fig. 1). Our study demonstrates that erosion led to a significant increase in the content and stock of SOC and its fractions at the lower zones, while depleting the carbon pool at the upper zones. The contents of both POC and MAOC decreased significantly with increasing soil depth, with a more pronounced reduction for POC; nevertheless, MAOC remained the dominant component of SOC (Fig. 1), underscoring its central role in maintaining carbon pool stability. Erosion exerted divergent effects on the different carbon fractions. POC, constituting a more labile carbon pool primarily derived from light, readily decomposable SOM, was particularly sensitive to erosion. Its significant reduction ($P < 0.05$) at the severely eroded upper zones is mainly attributable to its lower density and weaker aggregate protection, making it more susceptible to selective removal by runoff. This finding aligns with studies based on magnetic susceptibility, which identified convex slope shoulders as sites of the most severe soil loss due to runoff concentration (Liu et al., 2015). In contrast, MAOC, protected primarily through physicochemical sorption onto silt and clay mineral surfaces, exhibited greater stability and resistance to transport (He et al., 2023; Shi et al., 2024). During erosion-deposition events, runoff tends to preferentially transport fine particles (Han et al., 2021; Shi et al., 2025), leading to the loss of clay and silt from upper slopes and their enrichment at lower slopes (Chen et al., 2022; Hao et al., 2019). For instance, (Zhao et al., 2018) reported that most sediment eroded from sloping farmland is transported short distances and deposited at the foot-slope rather than being completely removed from the slope system. This redistribution of fine particles directly promotes MAOC accumulation at the lower slope by providing more mineral sorption sites. Furthermore, the spatial reorganization of unstable organic matter induced by erosion also profoundly influences SOC retention and turnover by regulating microbial mineralization processes (Xiao et al., 2017). In summary, erosion reshapes the soil carbon landscape along the slope through spatial redistribution: the upper slope experiences significant loss of the labile carbon pool (POC) due to physical removal and microenvironment degradation, while the lower zones promote the formation of a stabilized carbon pool dominated by MAOC through the deposition of transported carbon and fine particles.

4.2. Effects of erosion on extracellular enzyme activities and carbon use efficiency

Soil erosion reshaped the spatial distribution of extracellular enzyme activities (EEAs) and microbial carbon use efficiency (CUE) across the slope, primarily driven by the selective transport and deposition-induced redistribution of carbon fractions. In our study, the structural equation model revealed erosion as a key initial factor driving CUE variation, significantly influencing microbial metabolic function via indirect pathways (Fig. 7). CUE exhibited a clear spatial pattern, being significantly higher at the lower zones than at the upper zones in both

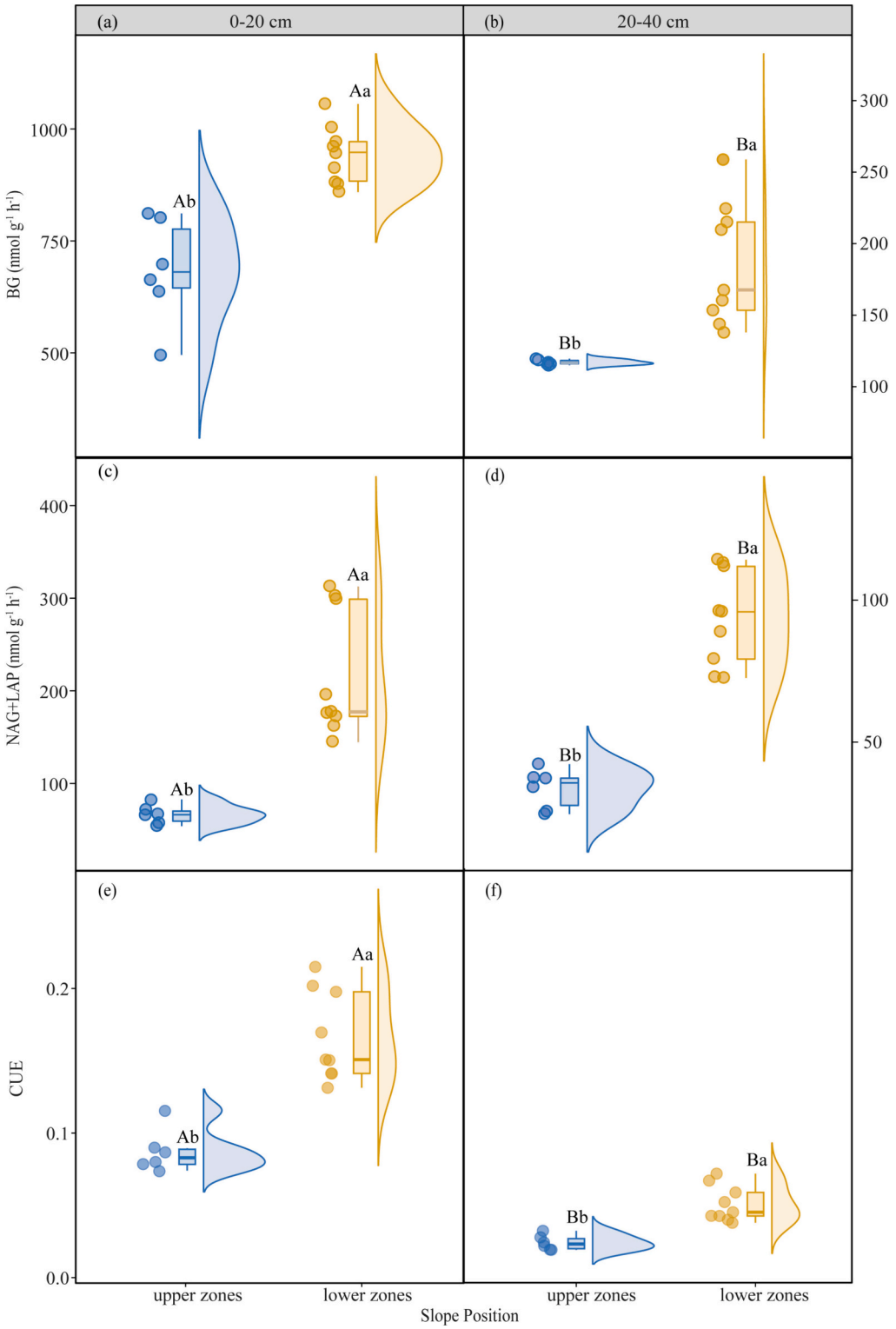

Fig. 3. S Vertical and lateral distribution of EEAs (a, b, c, d) and CUE (e, f) at different slope positions. BG: β-glucosidase; NAG+LAP: the sum of *N*-acetyl-β-glucosaminidase and leucine aminopeptidase; CUE: carbon use efficiency. Different capital letters indicate significant differences between distinct soil layers, while different lowercase letters indicate significant differences between distinct slope positions.

soil layers ($P < 0.05$, Fig. 3e, f). The erosion-induced decrease in CUE at the upper zones suggests a decline in soil carbon cycling efficiency, potentially increasing the risk of carbon loss as CO_2 (Fig. 6a) and weakening the ecosystem's carbon sequestration function.

Erosion further shaped microbial nutrient acquisition strategies by differentially regulating EEAs. As shown in Fig. 3, activities of BG and (NAG+LAP) were significantly higher at the lower zones compared to the severely eroded upper zones ($P < 0.05$). This spatial pattern, coupled with the elevated CUE at the lower zones, indicates a coordinated microbial response to the resource redistribution caused by erosion. At the depositional site, increased EEAs represent an investment strategy for nutrient acquisition from the accumulated SOM: The positive

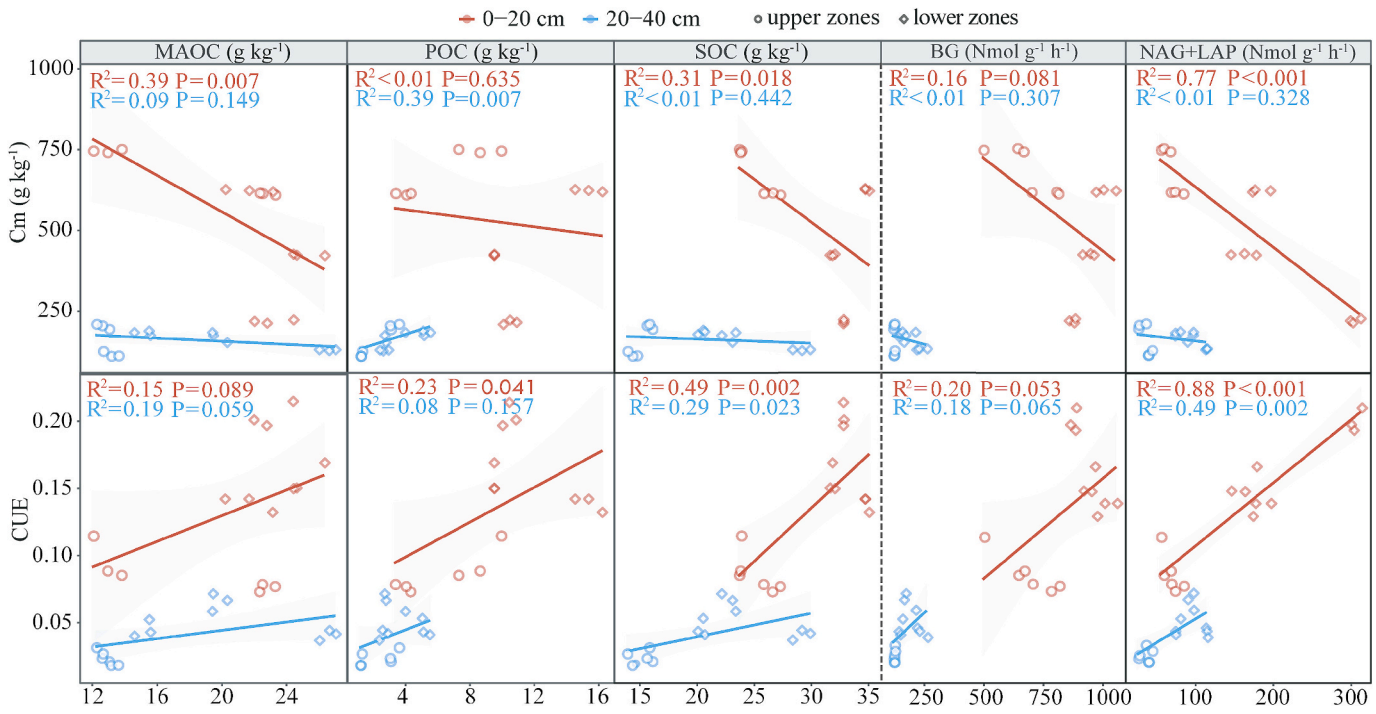

Fig. 4. Dependence of Cm and CUE on C fractions and EEAs. SOC: Soil organic carbon; POC: particulate organic carbon; MAOC: Mineral-associated organic carbon; BG: β-glucosidase; NAG+LAP: the sum of *N*-acetyl-β-glucosaminidase and leucine aminopeptidase; Cm: cumulative mineralization; CUE: carbon use efficiency.

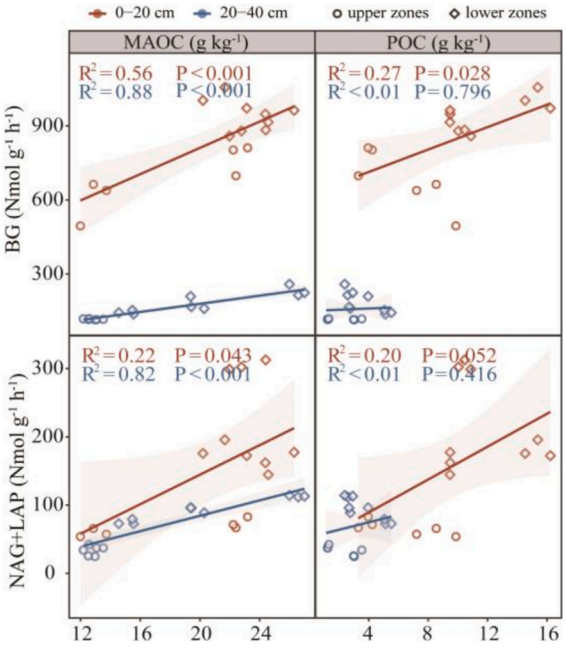

Fig. 5. Dependence of C fractions and EEAs. POC: particulate organic carbon; MAOC: Mineral-associated organic carbon; BG: β-glucosidase; NAG+LAP: the sum of *N*-acetyl-β-glucosaminidase and leucine aminopeptidase;

correlation between BG and POC ($P < 0.05$, Fig. 5) highlights that microbes prioritize decomposing labile POC via BG secretion to meet energy requirements, while the association between NAG+LAP and MAOC ($P < 0.05$, Fig. 5) suggests that microbial nitrogen acquisition relies on decomposing stable MAOC-bound nitrogen. This enzyme-substrate matching strategy is a key adaptive mechanism of microbial metabolism in eroded slopes. The higher CUE at the lower zones suggests that the energy gained from processing the abundant substrate (both POC and MAOC) outweighs the cost of enzyme production, leading to more efficient microbial growth. This promotes the conversion of assimilated carbon into microbial necromass, which is further stabilized as MAOC through sorption onto mineral surfaces and potentially enhancing SOC stability via the microbial carbon pump mechanism (Buckeridge et al., 2020a, 2020b; Wang et al., 2021). Conversely, at the eroded upper zones, depletion of fresh organic matter leads to resource limitation, shifting microbial metabolism towards maintenance rather than enzyme production, resulting in decreased enzyme activity, consistent with our previous findings (Li et al., 2024a). The lower CUE indicates a greater proportion of assimilated carbon is lost through respiration, representing a less efficient pathway for SOC accumulation (Fig. 7a) (Wang et al., 2024).

In the 0–20 cm layer, CUE was significantly positively correlated with POC and SOC ($P < 0.05$, Fig. 4), but not with MAOC. As an easily utilizable carbon source, POC provides readily available energy for microbes; the increased carbon accessibility significantly promotes microbial CUE and growth rate (Feng et al., 2022), indicating that the enhancement of CUE primarily depends on the input of labile carbon fractions rather than the stable carbon pool. This result supports the view that soil microbial CUE can indirectly regulate the dynamics of POC and MAOC through microbial biomass and necromass pathways, thereby influencing soil carbon storage (Yang et al., 2025). The strong correlation between CUE and SOC further highlights the critical link between microbial metabolic efficiency and the soil carbon pool. The nutrient-rich substrate deposited at the lower slope likely alleviates microbial nutrient limitation, enabling more efficient carbon use, a process regulated by the ecological stoichiometry of microbial carbon and nutrient metabolism. The coordinated increase in carbon-acquiring (BG) and nitrogen-acquiring (NAG+LAP) enzymes at the lower zones ensures a balanced supply of energy and nutrients, a key condition for maintaining high CUE.

On the other hand, erosion-induced carbon redistribution promoted microbial carbon capture efficiency to some extent, maintaining relatively higher CUE, particularly at the lower zones. While the overall CUE decreased in the 20–40 cm layer (Fig. 4) and the difference between slope positions narrowed, the spatial trend persisted, with the lower

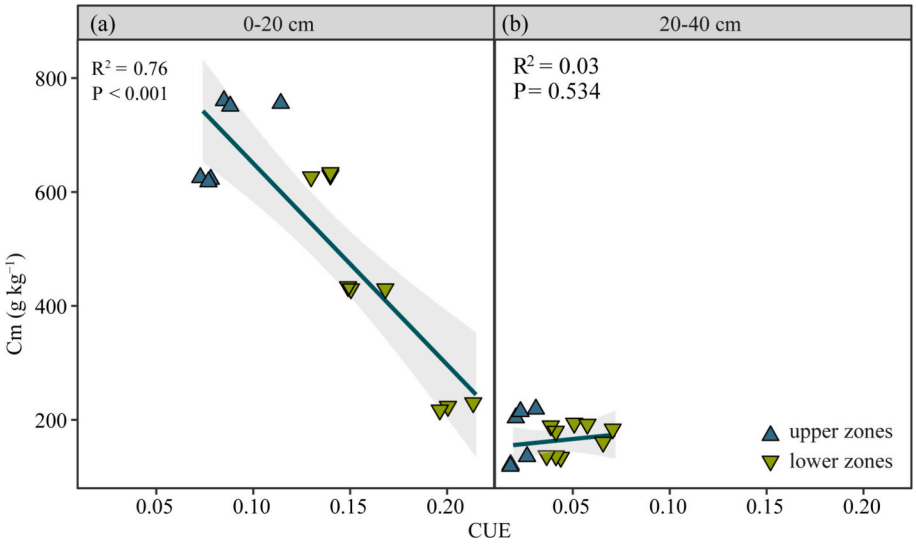

Fig. 5. The relationships between microbial CUE and Cm. Cm: cumulative mineralization; CUE: carbon use efficiency.

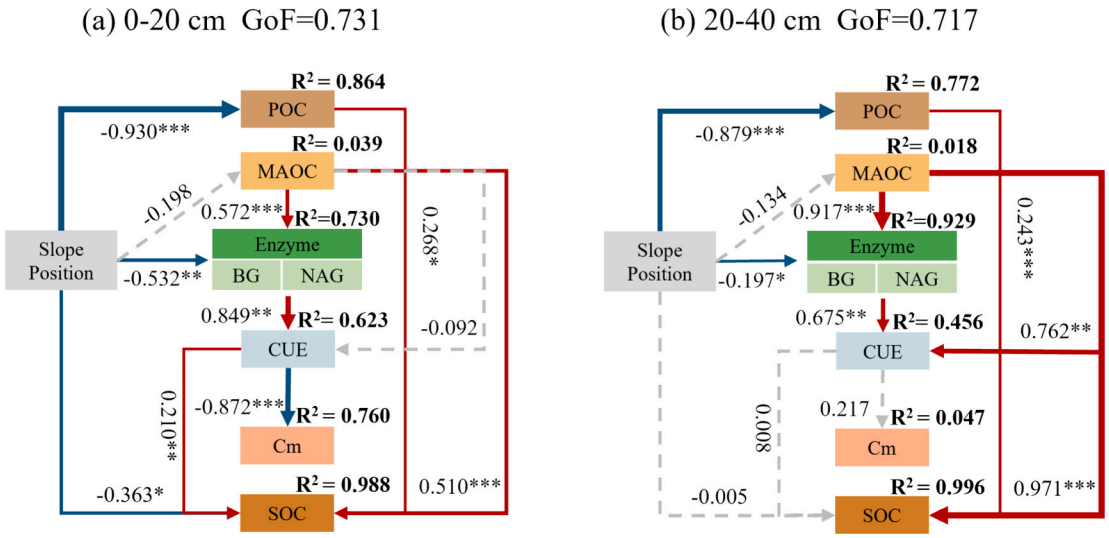

Fig. 7. Major pathways of soil carbon accumulation based on the partial least squares path modeling (PLS-PM). Numbers adjacent to arrows represent standardized path coefficients (*$P < 0.05$; ** $P < 0.01$; *** $P < 0.001$). The coefficient of determination (R^2) is displayed outside the variable boxes. The goodness-of-fit (GoF) index is indicated above the figure. C Fraction: POC, MAOC; POC: particulate organic carbon; MAOC: Mineral-associated organic carbon; Cm: cumulative mineralization; BG: β-glucosidase; NAG+LAP: the sum of *N*-acetyl-β-glucosaminidase and leucine aminopeptidase; CUE: carbon use efficiency. Blue and red arrows indicate positive and negative flows of causality, respectively. Grey dashed lines represent insignificant pathways. Numbers on the arrow indicate significant standardized path coefficients. The thicker the single arrow line the greater the effect on soil organic carbon and mineralization. The asterisks indicate the statistical significance (*$P < 0.05$; ** $P < 0.01$; *** $P < 0.001$). (For interpretation of the references to colour in this figure legend, the reader is referred to the web version of this article.)

zones maintaining a relatively higher CUE (Fig. 3f). The significant positive correlation between CUE and SOC, and between C_m and POC, in the subsoil indicates that labile organic carbon remains a key driver of microbial metabolism even at depth. However, the general decline in CUE with depth is likely associated with reduced input of labile carbon, the increasing dominance of the stable carbon pool (MAOC), and intensified energy limitation for microbes (He et al., 2025; Kan et al., 2020). As carbon availability decreases with depth, microbes allocate a greater proportion of carbon to respiration rather than growth, leading to a general decrease in microbial CUE (Zhang et al., 2023).

In conclusion, the spatial variation of CUE on the eroded slope is primarily regulated by the erosion-deposition-driven redistribution of carbon fractions. Upper zones lose labile carbon (e.g., POC), reducing microbial substrate availability and depressing CUE. Lower zones and subsoils have stable MAOC, providing a sustained energy base for microbes and supporting higher CUE. However, this study acknowledges a limitation that microbial community composition (e.g., shifts in fungi/bacteria ratio) may also influence CUE by altering substrate utilization strategies (Domeignoz-Horta et al., 2020). Future studies should integrate molecular techniques (e.g.,16S rRNA and Metagenomics sequencing) to quantify the relative contributions of substrate availability and microbial community composition to CUE dynamics (He et al., 2024).

4.3. Regulation of SOC accumulation by carbon fraction redistribution and microbial adaptation under erosion

Our study demonstrates that SOC accumulation and stability in sloping farmland are co-regulated by the spatial redistribution of carbon fractions triggered by physical transport and the subsequent adaptation

of microbial metabolism. Acting as the initial driver, erosion reshapes the distribution of the labile (POC) and stable (MAOC) carbon pools along the slope, inducing functional responses in microbes that ultimately lead to the formation of an effective carbon sink dominated by MAOC at the lower zones. This finding underscores the importance of partitioning SOC into POC and MAOC in erosion studies, as these fractions can reveal the underlying mechanisms of carbon dynamics more profoundly than bulk SOC (Angst et al., 2023; Lavallee et al., 2020; Rocci et al., 2021).

The PLS-PM (Fig. 7) clearly delineates the pathways and effects of various drivers. Erosion exerted a strong direct negative effect on SOC, with the greatest total negative effect on POC (Fig. 7a, b), confirming the role of the upper zones as a carbon "source". However, soil carbon fractions (POC and MAOC) exhibited significant positive total effects on SOC accumulation, indicating that carbon fraction redistribution is key to offsetting carbon loss (Li et al., 2022; Ning et al., 2021; Xiao et al., 2017). Regression analysis further revealed that MAOC explained more variation in C_m than POC or SOC, showing a significant negative correlation with C_m and a highly significant positive correlation with SOC content ($P < 0.05$, Fig. 4), confirming the dominant role of MAOC as a stable carbon pool in suppressing mineralization and promoting sequestration under erosion. This finding aligns with the global consensus that mineral protection is a dominant mechanism for long-term carbon sequestration (Angst et al., 2023; Cotrufo et al., 2019; Lugato et al., 2021).

CUE represents another crucial biological pathway linking carbon fractions to sequestration. The significant positive correlation between CUE and SOC in both soil layers ($P < 0.05$, Fig. 4) supports the "microbial carbon pump" theory, whereby higher CUE means more assimilated carbon is allocated to biomass synthesis rather than respiratory loss, thereby providing more stable input to the soil carbon pool (particularly for MAOC formation) through microbial necromass (Liang et al., 2017; Tao et al., 2023). The significant positive correlation between CUE and POC, but the lack thereof with MAOC ($P < 0.05$, Fig. 4), reflects the direct stimulatory effect of POC as a readily available energy source on microbial metabolism, and the biological inertness of MAOC due to its physicochemical protection by minerals.

Soil EEs play a pivotal role in this process, connecting carbon fractions to CUE as tools for microbial carbon acquisition. In our study, erosion affected carbon decomposition efficiency by reducing EEAs, while POC and MAOC, as substrate sources, stimulated the secretion of specific enzymes. Carbon fractions showed significant positive path coefficients towards EEAs, particularly MAOC, which had a stimulating effect on EEAs. Erosion had a direct negative path on EEAs, likely by directly altering microbial habitats and substrate availability through topsoil removal and aggregate disruption. Erosion primarily removes the labile carbon pool (POC), while the mineral-protected stable carbon pool (MAOC) is more erosion-resistant and serves as a major substrate source for extracellular enzymes, driving nutrient acquisition strategies. The negative correlation between Cm and CUE in the 0–20 cm layer (Fig. 6a) indicates that when microbes allocate more absorbed carbon to growth (high CUE), soil Cm decreases accordingly. This result reveals the key regulatory role of CUE in topsoil carbon sequestration from a microbial physiological ecology perspective (Liu et al., 2025b). In the subsoil, the mineralization of organic carbon is likely more limited by the chemical stability or physical accessibility of the carbon substrate, with the microbial carbon use strategy (CUE) having a relatively weaker influence.

The accumulation of MAOC is primarily controlled by the saturation of mineral sorption sites rather than microbial transformation efficiency. Microbial necromass (the product of CUE) needs to be associated with mineral surfaces to stabilize, a process constrained by clay content and iron/aluminum oxides, which inhibit microbial decomposition (King and Sokol, 2024; Liu et al., 2025a; Lv et al., 2023; Shi et al., 2024). Our results support the emerging theory that MAOC formation depends on the "saturation deficit" of mineral sorption sites and the existing MAOC stock, while CUE primarily supplies precursor materials (King and Sokol, 2025; Liang et al., 2017). The significant positive correlation between CUE and POC ($P < 0.05$, Fig. 4) confirms the attribute of POC as a "labile carbon pool", which is easily input but also easily lost. Composed of partially decomposed plant residues, POC is more readily utilized by microbes, whereas MAOC, sorbed to mineral surfaces, is less accessible due to mineral protection (Lavallee et al., 2020; Rocci et al., 2021). Consequently, POC is more sensitive to microbial action than MAOC. Although an increase in POC enhances carbon input, it does not effectively suppress mineralization. Lacking mineral protection, POC is susceptible to rapid microbial decomposition and may even prime the mineralization of native SOC (a positive priming effect).

In summary, the carbon dynamics on the eroded slope result from the synergy between physical transport and biological metabolism. The upper zones, experiencing the stripping of carbon fractions and suppression of microbial metabolism, acts as a carbon source. In contrast, the lower zones sequester carbon through the depositional enrichment of carbon fractions (especially MAOC) and efficient microbial conversion (high CUE). Efficient enzyme systems (e.g., high hydrolase activity for decomposable carbon) often coincide with higher CUE due to easier energy acquisition. Microbes enhance carbon use efficiency through these efficient systems, reducing respiratory losses and thereby promoting carbon sequestration. Physical transport by erosion causes carbon to migrate from high to low landscape positions, while microbial metabolic responses and mineral association mechanisms collectively determine the ultimate fate of the transported carbon, resulting in a dynamic redistribution pattern where carbon loss and sequestration coexist at the landscape scale.

We propose implementing contour cultivation to reduce the loss of POC and maintain the availability of microbial substrates, promoting no-till technology to preserve the accumulation of fine particles and enhance the mineral protection effect of MAOC, while applying organic amendments such as crop residues in upper zones to supplement the input of labile carbon and improve microbial CUE.

5. Conclusions

This study demonstrates that the competitive equilibrium governing SOC accumulation on slopes under soil erosion arises from the synergy between physical translocation and biological metabolic processes. Erosion induces selective removal of labile POC from upper zones, causing microbial substrate limitation and decreased CUE, thereby exacerbating carbon loss. Conversely, at lower zones, erosion facilitates the relative enrichment of stable MAOC through mineral protection mechanisms, establishing a local carbon sink. Simultaneously, vertical carbon migration contributes to the formation of a relatively stable MAOC pool in the subsoil (20–40 cm), partially offsetting the negative impacts of topsoil erosion. These processes result in a dynamic spatial trade-off between carbon loss and sequestration across the slope: severely eroded upper zones act as carbon sources, while lower zones function as carbon sinks via MAOC accumulation and microbial metabolic adaptation. This reveals that the carbon source/sink attribute of an eroded landscape is inherently governed by the spatial redistribution of carbon fractions and microbial metabolic responses. Future assessments of the carbon budget under soil erosion must concurrently quantify carbon losses from physical translocation and sequestration effects driven by mineral-biological synergy to systematically decipher the integrated response pathways of the carbon cycle to erosional disturbance.

CRediT authorship contribution statement

Mengni Li: Writing – review & editing, Writing – original draft, Visualization, Investigation, Formal analysis, Data curation, Conceptualization. **Yulong Shi:** Validation, Supervision, Investigation, Conceptualization. **Runyu Xue:** Validation, Investigation, Data curation. **Jeroen Meersmans:** Conceptualization, Supervision, Writing – review

& editing. **Qingwen Zhang:** Writing – review & editing, Supervision, Resources, Funding acquisition, Conceptualization.

Declaration of competing interest

The authors declare that they have no known competing financial interests or personal relationships that could have appeared to influence the work reported in this paper.

Acknowledgements

This work was supported by the Innovation Program of Chinese Academy of Agricultural Sciences (CAAS-CSAL-202302), and the National Natural Science Foundation of China (No. 41977072).

Data availability

Competitive Equilibrium Between Carbon Loss and Sequestration driven by Erosion: Stratified Responses of Microbial Metabolism and Mineral Protection (Original data) (Mendeley Data)

References

An, J., Zheng, F., Wang, B., 2014. Using 137Cs technique to investigate the spatial distribution of erosion and deposition regimes for a small catchment in the black soil region, Northeast China. CATENA 123, 243–251. https://doi.org/10.1016/j.catena.2014.08.009.

Angst, G., Mueller, K.E., Castellano, M.J., Vogel, C., Wiesmeier, M., Mueller, C.W., 2023. Unlocking complex soil systems as carbon sinks: multi-pool management as the key. Nat. Commun. 14, 2967. https://doi.org/10.1038/s41467-023-38700-5.

Berhe, A.A., Barnes, R.T., Six, J., Marín-Spiotta, E., 2018. Role of soil erosion in biogeochemical cycling of essential elements: carbon, nitrogen, and phosphorus. Annu. Rev. Earth Planet. Sci. 46, 521–548. https://doi.org/10.1146/annurev-earth-082517-010018.

Buckeridge, K.M., La Rosa, A.F., Mason, K.E., Whitaker, J., McNamara, N.P., Grant, H.K., Ostle, N.J., 2020a. Sticky dead microbes: rapid abiotic retention of microbial necromass in soil. Soil Biol. Biochem. 149, 107929. https://doi.org/10.1016/j.soilbio.2020.107929.

Buckeridge, K.M., Mason, K.E., McNamara, N.P., Ostle, N., Puissant, J., Goodall, T., Griffiths, R.I., Stott, A.W., Whitaker, J., 2020b. Environmental and microbial controls on microbial necromass recycling, an important precursor for soil carbon stabilization. Commun. Earth Environ. 1, 36. https://doi.org/10.1038/s43247-020-00031-4.

Chen, J., Xiao, W., Zheng, C., Zhu, B., 2020. Nitrogen addition has contrasting effects on particulate and mineral-associated soil organic carbon in a subtropical forest. Soil Biol. Biochem. 142, 107708. https://doi.org/10.1016/j.soilbio.2020.107708.

Chen, S., Zhang, G., Zhu, P., Wang, C., Wan, Y., 2022. Impact of slope position on soil erodibility indicators in rolling hill regions of Northeast China. CATENA 217, 106475. https://doi.org/10.1016/j.catena.2022.106475.

Cotrufo, M.F., Ranalli, M.G., Haddix, M.L., Six, J., Lugato, E., 2019. Soil carbon storage informed by particulate and mineral-associated organic matter. Nat. Geosci. 12, 989–994. https://doi.org/10.1038/s41561-019-0484-6.

Doetterl, S., Berhe, A.A., Nadeu, E., Wang, Z., Sommer, M., Fiener, P., 2016. Erosion, deposition and soil carbon: a review of process-level controls, experimental tools and models to address C cycling in dynamic landscapes. Earth Sci. Rev. 154, 102–122. https://doi.org/10.1016/j.earscirev.2015.12.005.

Domeignoz-Horta, L.A., Pold, G., Liu, X.-J.A., Frey, S.D., Melillo, J.M., DeAngelis, K.M., 2020. Microbial diversity drives carbon use efficiency in a model soil. Nat. Commun. 11, 3684. https://doi.org/10.1038/s41467-020-17502-z.

Feng, X., Qin, S., Zhang, D., Chen, P., Hu, J., Wang, G., Liu, Y., Wei, B., Li, Q., Yang, Y., Chen, L., 2022. Nitrogen input enhances microbial carbon use efficiency by altering plant–microbe–mineral interactions. Glob. Chang. Biol. 28, 4845–4860. https://doi.org/10.1111/gcb.16229.

Frey, S.D., Lee, J., Melillo, J.M., Six, J., 2013. The temperature response of soil microbial efficiency and its feedback to climate. Nat. Clim. Change 3, 395–398. https://doi.org/10.1038/nclimate1796.

Gao, H., Song, X., Wu, X., Zhang, N., Liang, T., Wang, Z., Yu, X., Duan, C., Han, Z., Li, S., 2024. Interactive effects of soil erosion and mechanical compaction on soil DOC dynamics and CO2 emissions in sloping arable land. CATENA 238, 107906. https://doi.org/10.1016/j.catena.2024.107906.

Han, Z., Li, J., Li, Y., Gu, X., Chen, X., Wei, C., 2021. Assessment of the size selectivity of eroded sediment in a partially saturated sandy loam soil using scouring experiments. CATENA 201, 105234. https://doi.org/10.1016/j.catena.2021.105234.

Hao, H., Wang, J., Guo, Z., Hua, L., 2019. Water erosion processes and dynamic changes of sediment size distribution under the combined effects of rainfall and overland flow. Catena 173, 494–504. https://doi.org/10.1016/j.catena.2018.10.029.

He, Y., Zhang, F., Yang, M., Li, X., Wang, Z., 2023. Insights from size fractions to interpret the erosion-driven variations in soil organic carbon on black soil sloping farmland, Northeast China. Agr Ecosyst Environ 343, 108283. https://doi.org/10.1016/j.agee.2022.108283.

He, X., Abs, E., Allison, S.D., Tao, F., Huang, Y., Manzoni, S., Abramoff, R., Bruni, E., Bowring, S.P.K., Chakrawal, A., Ciais, P., Elsgaard, L., Friedlingstein, P., Georgiou, K., Hugelius, G., Holm, L.B., Li, W., Luo, Y., Marmasse, G., Nunan, N., Qiu, C., Sitch, S., Wang, Y.-P., Goll, D.S., 2024. Emerging multiscale insights on microbial carbon use efficiency in the land carbon cycle. Nat. Commun. 15, 8010. https://doi.org/10.1038/s41467-024-52160-5.

He, C., Chen, J.-S., Han, S.-W., Liu, W.-S., Liu, W.-X., Oladele, O.P., Dang, Y.P., Lal, R., Zhao, X., Zhang, H.-L., 2025. Unraveling carbon mineralization patterns and mechanisms in conservation agriculture: a global synthesis and multi-point experiment. J. Clean. Prod. 493, 144900. https://doi.org/10.1016/j.jclepro.2025.144900.

Kallenbach, C.M., Frey, S.D., Grandy, A.S., 2016. Direct evidence for microbial-derived soil organic matter formation and its ecophysiological controls. Nat. Commun. 7, 13630. https://doi.org/10.1038/ncomms13630.

Kan, Z.-R., Ma, S.-T., Liu, Q.-Y., Liu, B.-Y., Virk, A.L., Qi, J.-Y., Zhao, X., Lal, R., Zhang, H.-L., 2020. Carbon sequestration and mineralization in soil aggregates under long-term conservation tillage in the North China plain. CATENA 188, 104428. https://doi.org/10.1016/j.catena.2019.104428.

King, A.E., Sokol, N.W., 2024. Soil carbon formation is promoted by saturation deficit and existing mineral-associated carbon, not by microbial carbon-use efficiency. Sci. Adv. 11, eadv9482. https://doi.org/10.1126/sciadv.adv9482.

King, A.E., Sokol, N.W., 2025. Soil carbon formation is promoted by saturation deficit and existing mineral-associated carbon, not by microbial carbon-use efficiency. Sci. Adv. 11, eadv9482. https://doi.org/10.1126/sciadv.adv9482.

Kramer, M.G., Chadwick, O.A., 2018. Climate-driven thresholds in reactive mineral retention of soil carbon at the global scale. Nat. Clim. Change 8, 1104–1108. https://doi.org/10.1038/s41558-018-0341-4.

Lal, R., 2003. Soil erosion and the global carbon budget. Environ. Int. 29, 437–450. https://doi.org/10.1016/S0160-4120(02)00192-7.

Lavallee, J.M., Soong, J.L., Cotrufo, M.F., 2020. Conceptualizing soil organic matter into particulate and mineral-associated forms to address global change in the 21st century. Glob. Chang. Biol. 26, 261–273. https://doi.org/10.1111/gcb.14859.

Li, J., Shangguan, Z., Deng, L., 2022. Free particulate organic carbon plays critical roles in carbon accumulations during grassland succession since grazing exclusion. Soil Tillage Res. 220, 105380. https://doi.org/10.1016/j.still.2022.105380.

Li, M., Li, X., Shi, Y., Jiang, Y., Xue, R., Zhang, Q., 2024a. Soil enzyme activity mediated organic carbon mineralization due to soil erosion in long gentle sloping farmland in the black soil region. Sci. Total Environ. 929, 172417. https://doi.org/10.1016/j.scitotenv.2024.172417.

Li, Z., Duan, X., Guo, X., Gao, W., Li, Y., Zhou, P., Zhu, Q., O'Donnell, A.G., Dai, K., Wu, J., 2024b. Microbial metabolic capacity regulates the accrual of mineral-associated organic carbon in subtropical paddy soils. Soil Biol. Biochem. 195, 109457. https://doi.org/10.1016/j.soilbio.2024.109457.

Li, M., Zhang, Q., Meersmans, J., Degré, A., 2025. Distribution patterns of SOC fractions and mineralization on sloping erosion-prone farmland in the black soil region. Int. Soil Water Conserv. Res. https://doi.org/10.1016/j.iswcr.2025.08.001.

Liang, C., Schimel, J.P., Jastrow, J.D., 2017. The importance of anabolism in microbial control over soil carbon storage. Nat. Microbiol. 2, 17105. https://doi.org/10.1038/nmicrobiol.2017.105.

Liu, L., Zhang, K., Zhang, Z., Qiu, Q., 2015. Identifying soil redistribution patterns by magnetic susceptibility on the black soil farmland in Northeast China. CATENA 129, 103–111. https://doi.org/10.1016/j.catena.2015.03.003.

Liu, Z., Gu, H., Yao, Q., Jiao, F., Liu, J., Jin, J., Liu, X., Wang, G., 2022. Microbial communities in the diagnostic horizons of agricultural isohumosols in Northeast China reflect their soil classification. CATENA 216, 106430. https://doi.org/10.1016/j.catena.2022.106430.

Liu, L., Yang, J., Wang, J., Yu, Q., Wei, C., Jiang, L., Huang, J., Zhang, Y., Jiang, Y., Zhang, H., Han, X., 2025a. Increase in mineral-associated organic carbon does not offset the decrease in particulate organic carbon under long-term nitrogen enrichment in a steppe ecosystem. Soil Biol. Biochem. 202, 109695. https://doi.org/10.1016/j.soilbio.2024.109695.

Liu, M., Lin, H., Li, J., 2025b. Are there links between nutrient inputs and the response of microbial carbon use efficiency or soil organic carbon? A meta-analysis. Soil Biol. Biochem. 201, 109656. https://doi.org/10.1016/j.soilbio.2024.109656.

Lugato, E., Lavallee, J.M., Haddix, M.L., Panagos, P., Cotrufo, M.F., 2021. Different climate sensitivity of particulate and mineral-associated soil organic matter. Nat. Geosci. 14, 295–300. https://doi.org/10.1038/s41561-021-00744-x.

Lv, J., Shi, J., Wang, Z., Peng, Y., Wang, X., 2023. Effects of erosion and deposition on the extent and characteristics of organic carbon associated with soil minerals in mollisol landscape. CATENA 228, 107190. https://doi.org/10.1016/j.catena.2023.107190.

Manzoni, S., Čapek, P., Mooshammer, M., Lindahl, B.D., Richter, A., Šantrůčková, H., 2017. Optimal metabolic regulation along resource stoichiometry gradients. Ecol. Lett. 20, 1182–1191. https://doi.org/10.1111/ele.12815.

Marriott, E.E., Wander, M.M., 2006. Total and labile soil organic matter in organic and conventional farming systems. Soil Sci. Soc. Am. J. 70, 950–959. https://doi.org/10.2136/sssaj2005.0241.

Mercer, G.D., Mickan, B.S., Gleeson, D.B., Walker, E., Krohn, C., Bühlmann, C.H., Ryan, M.H., 2025. Probing the pump: soil carbon dynamics, microbial carbon use efficiency and community composition in response to stoichiometrically-balanced compost and biochar. Soil Biol. Biochem. 205, 109770. https://doi.org/10.1016/j.soilbio.2025.109770.

Nelson, D.W., Sommers, L.E., 1996. Total carbon, organic carbon, and organic matter. In: Methods of soil analysis: part 3 chemical methods 5, pp. 961–1010. https://doi.org/10.2136/sssabookser5.3.c34.

Ning, Q., Hättenschwiler, S., Lü, X., Kardol, P., Zhang, Y., Wei, C., Xu, C., Huang, J., Li, A., Yang, J., Wang, J., Peng, Y., Peñuelas, J., Sardans, J., He, J., Xu, Z., Gao, Y., Han, X., 2021. Carbon limitation overrides acidification in mediating soil microbial activity to nitrogen enrichment in a temperate grassland. Glob. Chang. Biol. 27, 5976–5988. https://doi.org/10.1111/gcb.15819.

Ren, C., Zhou, Z., Delgado-Baquerizo, M., Bastida, F., Zhao, F., Yang, Y., Zhang, S., Wang, Jieying, Zhang, C., Han, X., Wang, Jun, Yang, G., Wei, G., 2024. Thermal sensitivity of soil microbial carbon use efficiency across forest biomes. Nat. Commun. 15, 6269. https://doi.org/10.1038/s41467-024-50593-6.

Report of the Protection and Utilization of Black Soil in China 2021, 2022. Chinese Academy of Science.

Rocci, K.S., Lavallee, J.M., Stewart, C.E., Cotrufo, M.F., 2021. Soil organic carbon response to global environmental change depends on its distribution between mineral-associated and particulate organic matter: a meta-analysis. Sci. Total Environ. 793, 148569. https://doi.org/10.1016/j.scitotenv.2021.148569.

Roels, J.A., 1980. Application of macroscopic principles to microbial metabolism. Biotechnol. Bioeng. 22, 2457–2514. https://doi.org/10.1002/bit.260221202.

Schimel, J., Weintraub, M.N., Moorhead, D., 2022. Estimating microbial carbon use efficiency in soil: isotope-based and enzyme-based methods measure fundamentally different aspects of microbial resource use. Soil Biol. Biochem. 169, 108677. https://doi.org/10.1016/j.soilbio.2022.108677.

Shen, Y., Gu, J., Liu, G., Wang, X., Shi, H., Shu, C., Zhang, Q., Guo, Z., Zhang, Y., 2023. Predicting soil erosion and deposition on sloping farmland with different shapes in Northeast China by using 137Cs. Catena 229, 107238.

Shi, J., Lv, J., Peng, Y., Yao, Y., Wei, X., Wang, X., 2024. Mechanisms controlling the stability and sequestration of mineral associated organic carbon upon erosion and deposition. CATENA 242, 108119. https://doi.org/10.1016/j.catena.2024.108119.

Shi, J., Zhang, Ziyun, Zhang, Zhiyong, Fan, Z., Wang, X., 2025. Erosion-induced low carbon availability exacerbates carbon loss: insights from microbial carbon allocation and the chemo-diversity of carbon. CATENA 252, 108894. https://doi.org/10.1016/j.catena.2025.108894.

Sorokin, A., Owens, P., Láng, V., Jiang, Z.-D., Michéli, E., Krasilnikov, P., 2021. "Black soils" in the russian soil classification system, the US soil taxonomy and the WRB: quantitative correlation and implications for pedodiversity assessment. CATENA 196, 104824. https://doi.org/10.1016/j.catena.2020.104824.

Tang, B., Rocci, K.S., Lehmann, A., Rillig, M.C., 2023. Nitrogen increases soil organic carbon accrual and alters its functionality. Glob. Chang. Biol. 29, 1971–1983. https://doi.org/10.1111/gcb.16588.

Tao, F., Huang, Y., Hungate, B.A., Manzoni, S., Frey, S.D., Schmidt, M.W.I., Reichstein, M., Carvalhais, N., Ciais, P., Jiang, L., Lehmann, J., Wang, Y.-P., Houlton, B.Z., Ahrens, B., Mishra, U., Hugelius, G., Hocking, T.D., Lu, X., Shi, Z., Viatkin, K., Vargas, R., Yigini, Y., Omuto, C., Malik, A.A., Peralta, G., Cuevas-Corona, R., Di Paolo, L.E., Luotto, I., Liao, C., Liang, Y.-S., Saynes, V.S., Huang, X., Luo, Y., 2023. Microbial carbon use efficiency promotes global soil carbon storage. Nature 618, 981–985. https://doi.org/10.1038/s41586-023-06042-3.

Wang, S., Zhao, Y., Wang, J., Gao, J., Zhu, P., Cui, X., Xu, M., Zhou, B., Lu, C., 2020. Estimation of soil organic carbon losses and counter approaches from organic materials in black soils of northeastern China. J. Soil. Sediment. 20, 1241–1252. https://doi.org/10.1007/s11368-019-02520-2.

Wang, B., An, S., Liang, C., Liu, Y., Kuzyakov, Y., 2021. Microbial necromass as the source of soil organic carbon in global ecosystems. Soil Biol. Biochem. 162, 108422. https://doi.org/10.1016/j.soilbio.2021.108422.

Wang, H., Yang, S., Wang, Y., Gu, Z., Xiong, S., Huang, X., Sun, M., Zhang, S., Guo, L., Cui, J., Tang, Z., Ding, Z., 2022. Rates and causes of black soil erosion in Northeast China. CATENA 214, 106250. https://doi.org/10.1016/j.catena.2022.106250.

Wang, Xiangxiang, Zhang, H., Cao, D., Wu, C., Wang, Xianting, Wei, L., Guo, B., Wang, S., Ding, J., Chen, H., Chen, J., Ge, T., Zhu, Z., 2024. Microbial carbon and phosphorus metabolism regulated by C:N:P stoichiometry stimulates organic carbon accumulation in agricultural soils. Soil Tillage Res. 242, 106152. https://doi.org/10.1016/j.still.2024.106152.

Xiao, H., Li, Z., Chang, X., Huang, J., Nie, X., Liu, C., Liu, L., Wang, D., Dong, Y., Jiang, J., 2017. Soil erosion-related dynamics of soil bacterial communities and microbial respiration. Appl. Soil Ecol. 119, 205–213. https://doi.org/10.1016/j.apsoil.2017.06.018.

Xu, X., Schimel, J.P., Janssens, I.A., Song, X., Song, C., Yu, G., Sinsabaugh, R.L., Tang, D., Zhang, X., Thornton, Peter.E., 2017. Global pattern and controls of soil microbial metabolic quotient. Ecol. Monogr. 87, 429–441. https://doi.org/10.1002/ecm.1258.

Yang, Y., Gunina, A., Cheng, H., Liu, L., Wang, B., Dou, Y., Wang, Y., Liang, C., An, S., Chang, S.X., 2025. Unlocking mechanisms for soil organic matter accumulation: carbon use efficiency and microbial necromass as the keys. Glob. Chang. Biol. 31, e70033. https://doi.org/10.1111/gcb.70033.

Ye, C., Chen, D., Hall, S.J., Pan, S., Yan, X., Bai, T., Guo, H., Zhang, Y., Bai, Y., Hu, S., 2018. Reconciling multiple impacts of nitrogen enrichment on soil carbon: plant, microbial and geochemical controls. Ecol. Lett. 21, 1162–1173. https://doi.org/10.1111/ele.13083.

Yu, W., Huang, W., Weintraub-Leff, S.R., Hall, S.J., 2022. Where and why do particulate organic matter (POM) and mineral-associated organic matter (MAOM) differ among diverse soils? Soil Biol. Biochem. 172, 108756. https://doi.org/10.1016/j.soilbio.2022.108756.

Zhang, X., Pei, G., Zhang, T., Fan, X., Liu, Z., Bai, E., 2023. Erosion effects on soil microbial carbon use efficiency in the mollisol cropland in Northeast China. Soil Ecol. Lett. 5, 230176. https://doi.org/10.1007/s42832-023-0176-4.

Zhang, S., Zhou, X., Chen, Y., Du, F., Zhu, B., 2024. Soil organic carbon fractions in China: spatial distribution, drivers, and future changes. Sci. Total Environ. 919, 170890. https://doi.org/10.1016/j.scitotenv.2024.170890.

Zhao, P., Li, S., Wang, E., Chen, X., Deng, J., Zhao, Y., 2018. Tillage erosion and its effect on spatial variations of soil organic carbon in the black soil region of China. Soil Tillage Res. 178, 72–81. https://doi.org/10.1016/j.still.2017.12.022.